

Dielectric Asymmetry in the Photosynthetic Reaction Center

Martin A. Steffen, Kaiqin Lao, Steven G. Boxer

Although the three-dimensional structure of the bacterial photosynthetic reaction center (RC) reveals a high level of structural symmetry, with two nearly equivalent potential electron transfer pathways, the RC is functionally asymmetric: Electron transfer occurs along only one of the two possible pathways. In order to determine the origins of this symmetry breaking, the internal electric field present in the RC when charge is separated onto structurally characterized sites was probed by using absorption band shifts of the chromophores within the RC. The sensitivity of each probe chromophore to an electric field was calibrated by measuring the Stark effect spectrum, the change in absorption due to an externally applied electric field. A quantitative comparison of the observed absorption band shifts and those predicted from vacuum electrostatics gives information on the effective dielectric constant of the protein complex. These results reveal a significant asymmetry in the effective dielectric strength of the protein complex along the two potential electron transfer pathways, with a substantially higher dielectric strength along the functional pathway. This dielectric asymmetry could be a dominant factor in determining the functional asymmetry of electron transfer in the RC.

The solution of the three-dimensional structure of the bacterial photosynthetic RC laid to rest many questions concerning the events that immediately follow absorption of a photon in photosynthesis (1, 2). One of the most surprising and puzzling discoveries was the observation of an approximate twofold axis of symmetry (Fig. 1). In spite of this structural symmetry, the light-driven primary electron transfer reactions take place only along one of the two potential branches of redox-active components (3, 4). This phenomenon has been named unidirectional electron transfer, and understanding its origin has generated much experimental and theoretical interest (3–7). To date, no convincing physical explanation has been provided. The significance of this problem extends beyond its obvious importance in photosynthesis, because there is widespread interest in understanding the factors that determine electron transfer rates in condensed phases (8), including proteins (9, 10). We present experimental evidence that the effective dielectric constant in the vicinity of the functional branch of components is considerably larger than that for the nonfunctional branch. This difference may be fundamentally related to the functional asymmetry of the RC because the enhanced dielectric screening along the functional pathway would stabilize charge-separated intermediates relative to those on the nonfunctional side.

The RC is comprised of two principal protein subunits, denoted L and M. Chro-

mophores that are primarily associated with these subunits are labeled with subscripts (Fig. 1). The functional branch of cofactors is along the L side, whereas the nonfunctional branch is along the M side. The secondary and tertiary structures of the L and M subunits are related by the approximate twofold axis of symmetry, and there is a moderately high level of sequence homology between them. Various attempts to increase the sequence homology, and therefore increase the symmetry of the RC, have led to many interesting results (11–16), but none has yet produced any evidence of a

deviation from unidirectional electron transfer. The absorption of light initiates the transfer of an electron from two closely interacting bacteriochlorophyll (BChl) molecules, referred to as the special pair and labeled P, to the bacteriopheophytin monomer (BPheo, in which the central Mg atom of BChl is replaced by 2H), labeled H_L , with some participation of the intervening BChl monomer B_L . The electron then moves from H_L^- to the quinone Q_A to form the state $P^+Q_A^-$, which has a lifetime of tens of milliseconds if quinone Q_B (not shown) is absent from the RC, as in the experiments discussed below.

We used the absorption bands of the BPheo (H_L and H_M) and BChl (B_L and B_M) chromophores as built-in probes of the internal electric field produced by the charge-separated $P^+Q_A^-$ state. We focus principally on the results obtained for H_L and H_M because the magnitude of excitonic coupling among various chromophores for the monomeric BChls is less well understood (see below). Upon formation of the internal electric field due to $P^+Q_A^-$, the BPheo absorption bands shift, a phenomenon often referred to as an electrochromic band shift. Although known for many years (17), these shifts have not been quantitatively analyzed. A quantitative analysis requires a determination of the sensitivity of individual absorption features to electric fields and a knowledge of the three-dimensional structure. Calibration of the field sensitivity is provided by a measurement of the Stark effect spectrum, and the distances and orientations of the probe chromophores are obtained from the x-ray structure.

Specifically, the magnitude of the elec-

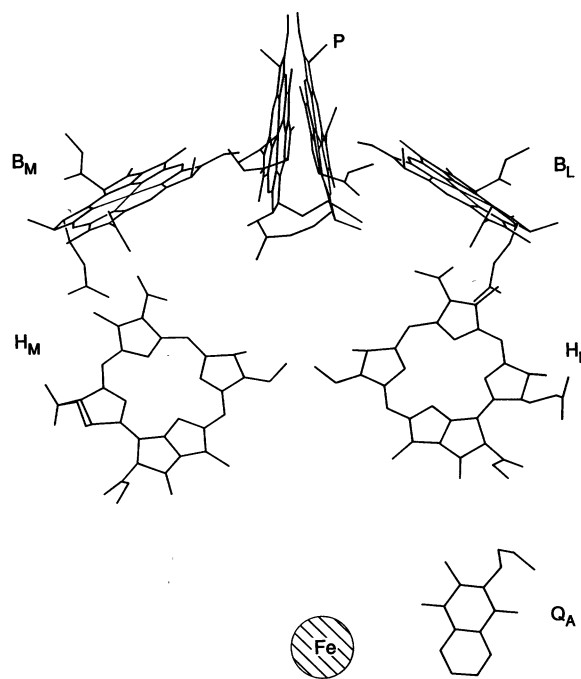


Fig. 1. Arrangement of the chromophores in the photosynthetic RC taken from the x-ray coordinates for *Rhodospseudomonas viridis* RCs (1, 2). A similar structure is observed for *Rhodobacter sphaeroides* (70, 71), where Q_A is ubiquinone.

The authors are in the Department of Chemistry, Stanford University, Stanford, CA 94305-5080, USA.

trichromatic band shift depends on two quantities: (i) the magnitude and direction of the difference in permanent dipole moment, $\Delta\mu$, for the BPheo monomer electronic transitions, and (ii) the magnitude and direction of the internal electric field, $F(P^+Q_A^-)$, produced by the charges on P^+ and Q_A^- at the positions of the probe BPheo chromophores. If θ is the angle between $\Delta\mu$ and $F(P^+Q_A^-)$, then the observed electrochromic band shift, $\Delta\nu_{\text{obs}}$, is given by:

$$\Delta\nu_{\text{obs}} = -|\Delta\mu| |F(P^+Q_A^-)| \cos\theta \quad (1)$$

The value of $\Delta\mu$ for each probe chromophore can be obtained by measuring the

effect of an external applied electric field, F_{ext} , on the absorption spectrum, also called the Stark effect spectrum (18–22). The magnitude and direction of the internal electric field at any position produced by P^+ and Q_A^- in vacuum ($\epsilon = 1$, where ϵ is the dielectric constant), $F_{\text{calc}}(P^+Q_A^-, \epsilon = 1)$, can be calculated from Coulomb's law by using the x-ray crystal structure coordinates and information on the P^+ and Q_A^- charge distributions from electron-nuclear double resonance (ENDOR) spectroscopy and theory (23):

$$F_{\text{calc}}(P^+Q_A^-, \epsilon = 1) = \sum_{i=1}^n \frac{q_i}{r_i^2} \hat{r}_i \quad (2)$$

where q_i is the partial charge on atom i , r_i is the vector between the charge q_i and the probe charge, and \hat{r}_i is a unit vector in the direction of r_i . We can use $F_{\text{calc}}(P^+Q_A^-, \epsilon = 1)$ to calculate the electrochromic band shift in vacuum, $\Delta\nu_{\text{calc}}(\epsilon = 1)$:

$$\Delta\nu_{\text{calc}}(\epsilon = 1) = -|\Delta\mu| |F_{\text{calc}}(P^+Q_A^-)| \cos\theta \quad (3)$$

The ability of a protein to screen charge decreases the magnitude of the electric field from the value calculated for $\epsilon = 1$, thereby reducing the magnitude of the observed band shift from the value calculated with Eq. 3. This difference can be characterized in terms of an effective dielectric constant, ϵ_{eff} , defined as the ratio of the calculated ($\epsilon = 1$) to the observed band shift:

$$\epsilon_{\text{eff}} = \frac{\Delta\nu_{\text{calc}}(\epsilon = 1)}{\Delta\nu_{\text{obs}}} \quad (4)$$

In the experiments discussed below, the band shifts predicted by vacuum electrostatics are compared with the experimentally determined electrochromic band shifts for H_L and H_M (see below for a discussion of B_L and B_M) that result when P and Q_A become charged, and the derived value of ϵ_{eff} is compared for chromophores on the L and M sides of the RC. A similar approach was used recently to measure the screening of charges along synthetic α helices (24).

Determination of $\Delta\nu_{\text{obs}}$. The absorption and steady-state $P^+Q_A^-$ -minus- PQ_A difference spectra (25) of the Q_y region of wild-type RCs (26) at 1.5 K are shown with solid lines in Fig. 2, A and C, respectively. In the difference spectrum, a small increase in absorption, thought to be due to P^+ , is seen on the low energy side of the spectrum. It appears as a flat positive baseline offset over a wide wavelength region. In order to obtain the absorption spectrum of RCs in the charge-separated state, $A(P^+Q_A^-)$, the magnitude of the bleach of the P band in the difference spectrum (Fig. 2C) was scaled to equal the maximum of the P absorption (Fig. 2A), the two were added together, and the flat baseline due to P^+ absorption was subtracted to yield the spectrum in Fig. 2D (27). This procedure assumes that there is no structure in the P^+ absorption between 740 and 830 nm (12,000 to 13,500 cm^{-1}); none is observed.

We now focus on the H-band region and assume that the spectral shifts observed when $P^+Q_A^-$ is formed are due exclusively to electrochromic effects. This assumption is strongly supported by the absence of absorption changes in the H-band region when P is in the triplet state (28, 29). Like P^+ , 3P has little oscillator strength in the 12,000 to 13,500 cm^{-1} region; however, 3P is uncharged so electrochromic shifts are negligible. Thus, the triplet-minus-singlet difference spectrum is specifically sensitive

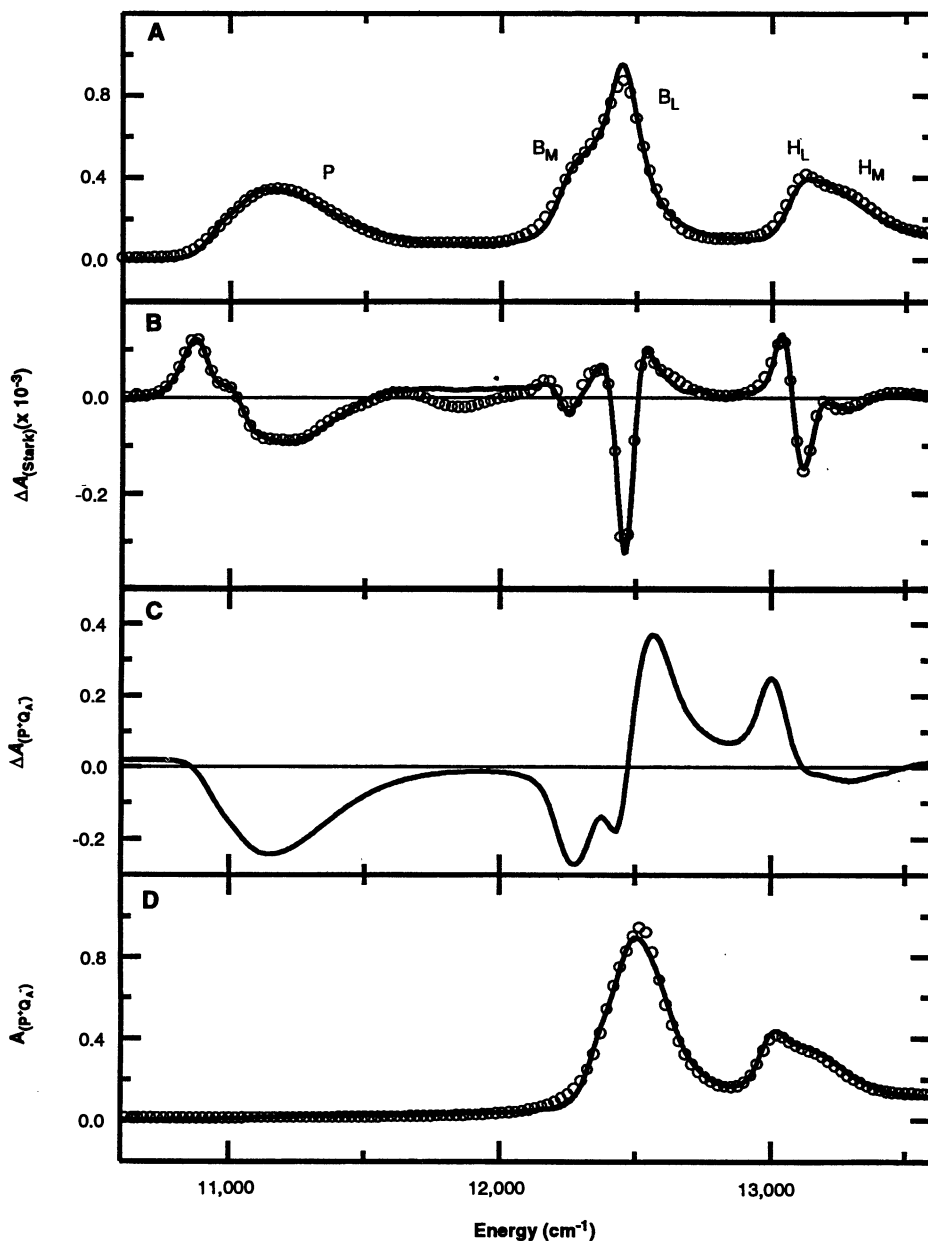


Fig. 2. (A) Absorption, (B) Stark effect ($|F_{\text{ext}}| = 9 \times 10^4$ V/cm, $\chi = 90^\circ$), (C) $P^+Q_A^-$ -minus- PQ_A difference absorption, and (D) $P^+Q_A^-$ absorption spectra in the Q_y region of wild-type *Rb. sphaeroides* RCs in a 50 percent (v/v) glycerol/buffer glass at 1.5 K. The solid lines are the data and the circles indicate the fits to the data.

to absorption changes associated with changes in excitonic coupling (28, 29). The absence of changes in the H bands demonstrates that changes in excitonic coupling with P are negligible for H_L and H_M , and therefore the observed band shifts in the $P^+Q_A^-$ state are likely entirely electrochromic in origin.

Expanded plots of the BPheo and BChl monomer region are shown in Fig. 3 with band assignments taken from previous studies (30). The two BPheo bands shift to lower energy upon formation of $P^+Q_A^-$, and the two BChl bands shift to higher energy (depicted by the arrows in Fig. 3). The signs of the spectral shifts imply that the angle between $F(P^+Q_A^-)$ and $\Delta\mu$ is $<90^\circ$ for the monomer BPheos, whereas the angle is $>90^\circ$ for the BChls (assuming the shifts are electrochromic in origin; see below). From the crystal structure, the observed signs of these spectral changes are consistent with the positive end of $\Delta\mu$ being closer to rings C and E of the macrocycle for all of the monomeric chromophores, as has been predicted by calculation (31).

In order to obtain $\Delta\nu_{\text{obs}}$, a method is needed to model quantitatively the absorption in the ground and $P^+Q_A^-$ states in the monomer region between 740 and 775 nm ($12,900$ to $13,500$ cm^{-1}). Because the absorption bands are clearly non-Gaussian, as expected for the absorption of an aromatic molecule, each band was treated simply as a sum of two Gaussians. Both Gaussians for each band were treated identically in subsequent analyses of the band shifts ($\Delta\nu_{\text{obs}}$) and Stark spectra (see below), and the same widths of the Gaussians were used to deconvolve the two absorption spectra (32). Most importantly, the deconvolution of the two absorption spectra was required to fit the Stark spectrum simultaneously (Fig. 2B; see below) so that the deconvolution is consistent with all of the experimental information used in the analysis of the band shifts. The best simultaneous fits to all of the data are shown with the open circles in Fig. 2, and the deduced band shifts are listed in Table 1. The H_M band exhibits a larger shift than its symmetry-related counterpart on the L side.

Determination of $\Delta\mu$. For an isotropic, immobilized sample, the line shape of the change in absorbance due to an externally applied electric field ΔA_{Stark} can be described by a sum of the zeroth, first, and second derivatives of the absorption spectrum (33–36). A second-derivative line shape dominates the Stark effect for the Q_y absorption bands of both isolated monomers (37) and the monomer bands in wild-type RCs (Fig. 2B) (38, 39). The open circles in Fig. 2B show the fit to the Stark spectrum that was obtained by using the

Table 1. Experimental and calculated parameters for analysis of electrochromic band shifts associated with the formation of the state $P^+Q_A^-$.

Parameter	Chromophore			
	B_M	H_M	B_L	H_L
Absorption position (cm^{-1})	12,271	13,268	12,452	13,113
$A(P^+Q_A^-)$ position (cm^{-1})	12,447	13,158	12,529	13,011
$\Delta\nu_{\text{obs}}$ (cm^{-1})	176	-110	77	-102
$ \Delta\mu $ (D/f)	2.5	2.7	2.9	3.3
ζ_A (degrees)	30	36	15	28
$ F_{\text{calc}}(P^+Q_A^-) $ (V/m)	7.6×10^8	4.5×10^8	1.1×10^9	1.2×10^9
θ (degrees)	144	31	134	47
$\Delta\nu_{\text{calc}}$ (cm^{-1})	260	-176	367	-465
ϵ_{eff}	1.5	1.6	4.7	4.5
Range (67)	0.7–1.8	0.9–1.7	3.3–5.9	2.5–5.1

same spectral decomposition used to fit the ground and $P^+Q_A^-$ absorption spectra.

The absolute directions of $\Delta\mu$ in the molecular axis system are also needed for the analysis of the band shifts. Precise experimental values for the directions in the RC are difficult to obtain for several reasons: first, the determination of ζ_A (35) only provides the projection of $\Delta\mu$ on the transition moment \mathbf{p} ; second, the direction of \mathbf{p} is not precisely known relative to the molecular axes, either for isolated monomeric BChl and BPheo or for these chromophores in the RC (40); and third, the measurement of the direction of $\Delta\mu$, although straightforward, can give misleading results for overlapping bands (41). We approach the uncertainty in the direction of $\Delta\mu$ as follows. In order to provide a frame of reference, the direction of \mathbf{p} is taken to lie along the line connecting the nitrogen atoms of rings A and C. This direction is close to that obtained by calculation and is consistent with linear dichroism measurements (42). We first fix $\Delta\mu$ to be parallel to \mathbf{p} ($\zeta_A = 0^\circ$), with the positive end of the difference dipole in the direction of ring C (consistent with the sign of the electrochromic band shifts). Next, the direction of $\Delta\mu$ was varied $\pm\zeta_A$ in the plane of each macrocycle by using the apparent value of ζ_A measured for each band in the RC at 77 K. This approach yields the widest reasonable range for the direction of $\Delta\mu$. Values of ζ_A measured for the isolated BChl and BPheo monomers in polymer matrices are not complicated by overlapping bands and are smaller [BPheo: $\zeta_A = 10^\circ$; BChl: $\zeta_A = 12^\circ$, see (21)] than the apparent values of ζ_A obtained for the overlapping bands in the RC, so it is very likely that the actual orientation of $\Delta\mu$ for the monomer bands in the RC is contained within the range of orientations sampled. There is no experimental evidence in any system which suggests that $\Delta\mu$ lies outside of these ranges. As shown below, regardless of the precise

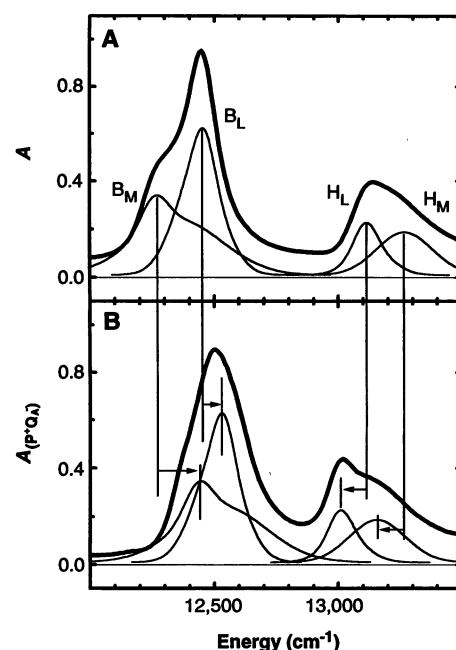


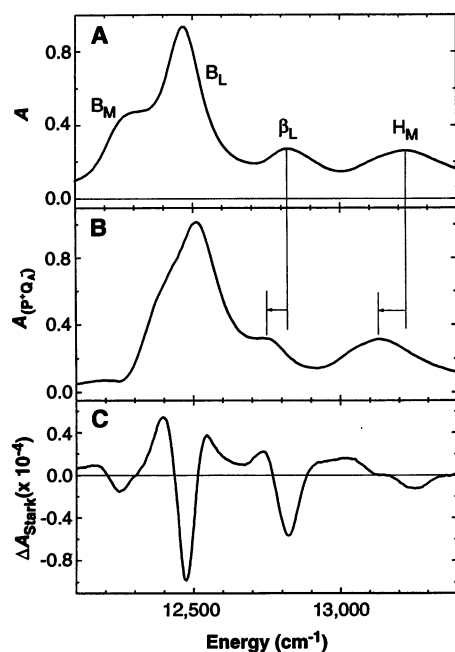
Fig. 3. Expanded view in the monomer region from Fig. 2 of (A) the ground-state absorption and (B) the $P^+Q_A^-$ absorption spectra of wild-type *Rb. sphaeroides* RCs. The dark solid curves are the data; the thinner lines are a deconvolution of the absorption assuming that only four species contribute to the absorption in this region (monomeric B_M , B_L , H_M , and H_L) and that each chromophore's non-Gaussian absorption profile can be approximated by a sum of two Gaussians (see text). The identical components (amplitudes and linewidths) are shifted in (B) to obtain $\Delta\nu_{\text{obs}}$, which is illustrated with the arrows and vertical lines (see Table 1).

orientation of $\Delta\mu$ within this range, the qualitative results for our estimates of ϵ_{eff} are unaffected.

Determination of $F_{\text{calc}}(P^+Q_A^-)$, $\epsilon = 1$. The direction and magnitude of the field $F_{\text{calc}}(P^+Q_A^-)$ at the center of each probe chromophore assuming $\epsilon = 1$ (vacuum) can be calculated with Coulomb's law (Eq. 2). The charge density distribution for P^+ is

Table 2. Experimental and calculated parameters for the analysis of electrochromic band shifts associated with the formation of the singly charged states P^+ and Q_A^-

Parameter	P^+				Q_A^-
	B_M	H_M	B_L	H_L	H_L
$\Delta\nu_{\text{obs}}$ (cm^{-1})	110	-60	34	-25	-50
$ \Delta\mu $ (D/f)	2.5	2.7	2.9	3.3	3.3
ζ_A (degrees)	30	36	15	28	28
$ F_{\text{calc}} $ (V/m)	8.3×10^8	4.2×10^8	9.7×10^8	8.9×10^8	8.9×10^8
θ (degrees)	143	50	132	47	54
$\Delta\nu_{\text{calc}}$ (cm^{-1})	276	-123	320	-174	-290
ϵ_{eff}	2.5	2.1	9.5	6.8	5.8
Range	1.3–3.0	0.2–3.2	6.8–11.6	2.6–9.5	3.8–6.4

**Fig. 4.** (A) Absorption, (B) $P^+Q_A^-$ absorption, and (C) Stark effect ($|F_{\text{ext}}| = 4.5 \times 10^4$ V/cm, $\chi = 90^\circ$) spectra in the monomer Q_y region of (M)L214H (β mutant) *Rb. sphaeroides* RCs in a 50 percent (v/v) glycerol/buffer glass at 1.5 K.

based on the analysis of ENDOR spectra and quantum mechanical calculations (23). A simpler alternative is to place a point charge at the geometric center of P; however, this overestimates the field at B_L and B_M by nearly 25 percent, because the entire field originates from a single point in space. If one uses the more realistic distribution of partial positive charges over the two macrocycles, the field is decreased by the cancelling of components perpendicular to the final direction of the field. The results are not very sensitive to the details of the charge distribution on the macrocycles, and similar results are obtained if the positive charge is simply distributed evenly over the two macrocycles. The location of the negative charge on Q_A^- is taken as the geometric center of the atoms contributing to the conjugated π system. Relative to the charge on P^+ , the spatial extent of the

charge on Q_A^- is smaller, and its distance from the other chromophores is greater, such that the consequences of approximating the location of the charge at a single point were relatively minor. The values of $F_{\text{calc}}(P^+Q_A^-, \epsilon = 1)$ range from 4.5×10^8 to 1.2×10^9 V/m and are presented in Table 1 for each probe chromophore.

Band shifts in (M)L214H RCs. Absorption spectra in the monomer region are shown in Fig. 4, A and B, for the neutral ground and $P^+Q_A^-$ states, respectively, of the β mutant RC (Leu^{M214} \rightarrow His) (43). The ground-state spectrum shows the improved spectral resolution when a BChl replaces BPheo in the H_L binding site. As was the case for wild-type RCs, the two B bands shift to higher energy and the H_M and β_L bands shift to lower energy upon formation of $P^+Q_A^-$. The shift for the H_M band is somewhat larger than for the β_L band, as illustrated with the vertical lines and arrows. The β_L band shows a large second-derivative Stark signal (Fig. 4C).

Chemical oxidation of P and reduction of Q_A^- . The band shifts that occur when P is chemically oxidized to P^+ (44) were investigated to rule out the possibility that any of the observed asymmetry in ϵ_{eff} was a consequence of electron transfer occurring down the L side when $P^+Q_A^-$ is formed (45). The absorption spectra of wild-type RCs in the presence of either 400 mM KCl or 400 mM $K_3Fe(CN)_6$, which oxidizes P to P^+ , were measured, and the absorption spectra were deconvolved as described above. The spectra are similar to those at higher temperatures (44). The spectral shifts for P^+ RCs are summarized in the first four columns of Table 2.

As a complement to the chemical oxidation of P, the band shifts that occur when Q_A is reduced to Q_A^- with sodium dithionite (44) were investigated. Because Q_A absorbs in the near ultraviolet, the band shifts in the near infrared due to Q_A^- contain no significant contributions from changes in excitonic coupling. Absorption spectra were obtained in the presence of 20 mM sodium chloride or 20 mM sodium dithionite, again giving spectra similar to

those reported previously (44), and the spectra were deconvolved as described above. The only significantly shifted absorption band is that of H_L , as expected given the close proximity of H_L and Q_A , summarized in the last column of Table 2.

Calculation of ϵ_{eff} . The data for RCs from the β mutant provide an exceptionally clear example of the asymmetry in ϵ_{eff} by direct inspection. The Stark effect spectrum in Fig. 4C shows that $|\Delta\mu|$ for β_L is considerably larger than for H_M (this result is confirmed by a quantitative analysis). Thus, the β_L band is more sensitive to an electric field than the H_M band, and for identical values of the field the β_L electrochromic band shift should be substantially larger. Furthermore, inspection of the x-ray structure in Fig. 1 shows that the field produced by $P^+Q_A^-$ should be larger at the β_L (or H_L) site than the H_M site because the charges on P^+ and Q_A^- are closer [see Table 1 for $F_{\text{calc}}(P^+Q_A^-)$ for the quantitative analysis]. Thus, these factors lead to the prediction that the electrochromic band shift for β_L in the presence of $P^+Q_A^-$ should be substantially larger than for H_M in vacuum. In contrast, comparison of Fig. 4, A and B, shows that the electrochromic band shift for β_L is smaller than the band shift for H_M (this result is confirmed by a quantitative analysis in which the procedure discussed in detail for wild-type RCs is used). The implication is that the protein dielectric screening of the charges on P^+ and Q_A^- is considerably larger on the L side than it is on the M side.

Inspection of the data for wild type in Figs. 2 and 3 leads to a similar qualitative conclusion. Because wild-type RCs have been much more thoroughly studied and characterized, we restrict the quantitative analyses to wild-type RCs. Table 1 summarizes the calculation of ϵ_{eff} for the optically prepared $P^+Q_A^-$ state (45). Table 2 summarizes the calculation for the chemically prepared P^+ and Q_A^- states. The orientation of $\Delta\mu$ is treated as discussed in detail above, and ϵ_{eff} is calculated according to Eq. 4. As can be seen, the range of estimates for ϵ_{eff} is consistently higher on the L side than for the M side.

Analysis of band shifts for the monomeric BChls. In principle, independent information can be obtained by an analysis of the band shifts in the B band region (12,100 to 12,800 cm^{-1} ; 780 to 825 nm). If we adopt the view that the excitonic contribution is small relative to the electrochromic contribution, we can perform the same quantitative analysis as for the H bands (46–49). The results are summarized in Tables 1 and 2 and yield estimates for both the asymmetry in ϵ_{eff} and for the absolute magnitudes of ϵ_{eff} which are similar to those for the H bands (50). As discussed

elsewhere in detail (51), the absorption spectra of the B and H monomer bands change much less when the absorption spectrum of P is changed drastically, for example, in the heterodimer mutant (His^{M200} → Leu) (52) or upon chemical modification of the B or H chromophores (51), than when P⁺Q_A⁻ is formed. Furthermore, if the B and P absorption band positions had a significant contribution from exciton interactions between B and P, then the loss of this exciton splitting upon formation of P⁺ would be expected to shift the absorption of B to lower, not higher, energy because the splitting is removed. Additionally, for identical chromophores at nearly identical distances and relative orientations, excitonic coupling should be nearly equal, producing splittings of similar magnitudes. We observe band shifts of very different magnitude for the two sides. These experimental data argue that both the H and B absorption band positions are not strongly affected by exciton interactions with P, supporting the hypothesis that the band shifts observed for both sets of chromophores upon formation of P⁺Q_A⁻ and P⁺ are largely electrochromic in origin. These data contrast with the results of some quantum chemical calculations of the absorption spectrum (53–55), but, as discussed in (51), this conclusion is far from unanimous.

Implications for RC function. All else being equal, the higher effective dielectric constant on the L side implies that the energy of the key charge-separated states, such as P⁺B_L⁻ and P⁺H_L⁻, will be lower on the L side than the M side because the ion pairs will be more strongly solvated. This experimental result is consistent with the conclusion of theoretical studies which suggest that the higher energy of charge-separated states on the M side is one of the primary determinants of the unidirectionality of electron transfer in the RC (56–59). The obvious next question is to determine which amino acids are responsible for the dielectric asymmetry. Attempts to symmetrize the environment around the special pair (14, 15), the amino acids in the vicinity of the entire electron transport chain (12), and residues that clearly break the symmetry, such as Tyr^{M210} (13, 16) and Glu^{L104} (11), have not shown evidence for electron transport down the M side. We have investigated the electrochromic band shifts for the Tyr^{M210} → Phe mutant and obtained results that are similar to those of the wild type for the shifts of the two BPheo bands. We conclude that many small contributions, including those from amino acids that are quite distant from the redox-active components, combine to give a substantial dielectric, and therefore functional, asymmetry. A similar view emerges from

molecular dynamics simulations, which suggest, in one case, that 20 amino acid residues participate in the solvation of P⁺H_L⁻ (58). These studies, as well as the relative insensitivity of the initial electron transfer to single-site mutations, suggest that the molecular explanation for the functional asymmetry of the photosynthetic RC is due to collective properties of a large portion of the protein complex. It is unlikely that any individual amino acid residue is alone responsible for the dielectric asymmetry, so the challenge of forcing electrons to transfer down the nonfunctional M side may be difficult to achieve.

An examination of the polarity of the amino acid residues that are within 7 Å of either H_L and H_M (60), as measured by their hydrophathy (61), reveals a previously unrecognized asymmetry in polarity that mirrors the observed dielectric asymmetry. The asymmetry persists when distances less than 7 Å are used as a cutoff; residues further than 7 Å are also expected to contribute, but were not considered here. The residues that primarily account for the asymmetry in polarity tend to be located near the edges of the macrocycles, whereas the polarity of the residues located above and below the macrocycle tend to be more or less equal. A similar asymmetry in polarity is observed for residues within 7 Å of the two BChl molecules that comprise the special pair, P_L and P_M. The differences in polarity are not restricted to a few amino acid residues near the chromophores. Twelve residues are more polar near H_L, and nine residues are more polar near P_L. No asymmetry of polarity is found for the residues near B_L and B_M in *Rhodobacter sphaeroides*; however, a similar analysis reveals an even more pronounced asymmetry in the polarity of amino acid residues around all of the symmetry-related chromophores in *Rhodospseudomonas viridis*.

Spatial variation of the dielectric constant, in particular an asymmetry between the two branches as suggested by this study, could also have significant consequences for electronic coupling matrix elements. This possibility has received only limited discussion in the photosynthesis field (62) and in electron transfer work in general (63–66). The simple concept is that the barrier height for electron tunneling may decrease with increasing dielectric constant, thereby increasing orbital overlap and enhancing the electronic coupling between reactant and product states (65, 66). If this effect is significant, it implies that, all else being equal, the electronic coupling will be greater along the L pathway, although the quantitative magnitude of the effect needs to be considered theoretically.

The absolute values of ε_{eff} support the notion of a low dielectric interior in the RC

at 1.5 K; however, they are subject to the greatest cumulative experimental error (67). Most of these uncertainties do not affect the relative value of ε_{eff} on the L and M sides, which is the central result of this study. Because of the loss of spectral resolution that accompanies thermal band broadening, the individual bands cannot be reliably deconvolved at higher temperatures [even for the β mutant (43)], and therefore no information can be obtained regarding dielectric asymmetry at room temperature. However, by treating the monomeric H bands as a unit, we can estimate the average band shift. If we compare the average shift at 1.5, 77, and 298 K, we find little difference between 1.5 and 77 K, but a significant decrease (~45 percent) in the magnitude of the average band shift at 298 K. This result indicates that the dielectric strength of the protein nearly doubles between 77 and 298 K, which is consistent with other measurements on the RC (68). The unidirectionality of electron transfer in the RC is independent of temperature (69), so the conclusions reached here regarding asymmetry can likely be transferred to physiological conditions.

REFERENCES AND NOTES

- J. Deisenhofer, O. Epp, K. Miki, R. Huber, H. Michel, *J. Mol. Biol.* **180**, 385 (1984).
- _____, *Nature* **318**, 618 (1985).
- D. J. Lockhart, C. Kirmaier, D. Holten, S. G. Boxer, *J. Phys. Chem.* **94**, 6987 (1990).
- C. Kirmaier, D. Holten, W. W. Parson, *Biochim. Biophys. Acta* **810**, 49 (1985).
- M. E. Michel-Beyerle *et al.*, *ibid.* **932**, 52 (1988).
- M. Plato, K. Möbius, M. E. Michel-Beyerle, M. Bixon, J. Jortner, *J. Am. Chem. Soc.* **110**, 7279 (1988).
- P. O. J. Scherer and S. F. Fischer, *J. Phys. Chem.* **93**, 1633 (1989).
- G. L. Closs and J. R. Miller, *Science* **240**, 440 (1988).
- D. N. Beratan, J. N. Onuchic, J. B. Betts, B. E. Bowler, H. B. Gray, *J. Am. Chem. Soc.* **112**, 7915 (1990).
- C. C. Moser, J. M. Keske, K. Warncke, R. S. Farid, P. L. Dutton, *Nature* **355**, 796 (1992).
- E. J. Bylina, C. Kirmaier, L. McDowell, D. Holten, D. C. Youvan, *ibid.* **336**, 182 (1988).
- S. J. Robles, J. Breton, D. C. Youvan, *Science* **248**, 1402 (1990).
- V. Nagarajan, W. W. Parson, D. Gaul, C. Schenck, *Proc. Natl. Acad. Sci. U.S.A.* **87**, 7888 (1990).
- J. W. Stocker, A. K. Taguchi, H. A. Murchison, N. W. Woodbury, S. G. Boxer, *Biochemistry* **31**, 10356 (1992).
- J. C. Williams *et al.*, *ibid.*, p. 11029.
- M. Du *et al.*, *Proc. Natl. Acad. Sci. U.S.A.* **89**, 8517 (1992).
- J. R. Bolton, R. K. Clayton, D. W. Reed, *Photochem. Photobiol.* **9**, 209 (1969).
- D. DeLeeuw, M. Malley, G. Butterman, M. Y. Okamura, G. Feher, *Biophys. Soc. Annu. Meet. Abstr.* **37**, 111a (1982).
- D. J. Lockhart and S. G. Boxer, *Biochemistry* **26**, 664 (1987); *ibid.*, p. 2958.
- M. Lösche, G. Feher, M. Y. Okamura, *Proc. Natl. Acad. Sci. U.S.A.* **84**, 7537 (1987).
- D. J. Lockhart and S. G. Boxer, *ibid.* **85**, 107 (1988).
- M. Lösche, G. Feher, M. Y. Okamura, in *The Photosynthetic Bacterial Reaction Center—Structure and Dynamics*, J. Breton and A. Vermeglio,

- Eds. (Plenum, New York, 1988), pp. 151–164.
23. M. Plato, K. Möbius, W. Lubitz, J. P. Allen, G. Feher, in *Perspectives in Photosynthesis*, J. Jortner and B. Pullman, Eds. (Kluwer Academic, Dordrecht, Netherlands, 1990), pp. 423–434.
 24. D. J. Lockhart and P. S. Kim, *Science* **257**, 947 (1992).
 25. Transmission spectra of the samples and a blank at 1.5 K were obtained to yield the absorption spectra. Transmission spectra of the RC samples with and without steady-state illumination from an argon-ion laser (0.5 W/0.25 cm² at 514 and 488 nm) were used to obtain the P⁺Q_A⁻-minus-PQ_A (light minus dark) difference absorption spectra.
 26. Wild-type (carotenoid-containing) *Rhodospirillum rubrum* were grown semiaerobically. The RCs were obtained by standard methods, with final purification by chromatography at moderate pressure on DEAE Toyopearl 650S. The RCs, dissolved in 0.025 percent lauryl-dimethylamine-oxide (LDAO) detergent, 10 mM tris, pH 8, 10 mM NaCl, were diluted with glycerol to a final solvent composition of 50% (v/v) glycerol/buffer.
 27. The difference spectrum in Fig. 2C is the more common way of presenting the data, in part, because it emphasizes the changes in the spectrum. However, it is misleading to refer to the features at 12,300, 12,450, and 12,600 cm⁻¹ as bands that are disappearing or growing in. Comparison of Fig. 2, A and D, demonstrates that band shifts can explain the observed changes in absorption in this region, and that no new bands need be invoked.
 28. E. J. Lous and A. J. Hoff, *Biochim. Biophys. Acta* **974**, 88 (1989).
 29. A. J. Hoff, E. J. Groenen, E. J. Lous, in *Perspectives in Photosynthesis*, J. Jortner and B. Pullman, Eds. (Kluwer Academic, Dordrecht, Netherlands, 1990), pp. 71–80.
 30. J. Breton, in *The Photosynthetic Bacterial Reaction Center—Structure and Dynamics*, J. Breton and A. Vermeglio, Eds. (Plenum, New York, 1988), pp. 59–69.
 31. J. Fajer, L. K. Hanson, M. C. Zerner, M. A. Thompson, in *The Photosynthetic Bacterial Reaction Center II—Structure, Spectroscopy and Dynamics*, J. Breton and A. Vermeglio, Eds. (Plenum, New York, 1992), pp. 33–42.
 32. A very broad Gaussian band, extending over the entire Q_y spectral region, was used in the fitting procedure to model the baseline. This band contributed identically to the two absorption spectra; it was not allowed to shift.
 33. S. G. Boxer, in *The Photosynthetic Reaction Center*, J. Deisenhofer and J. R. Norris, Eds. (Academic Press, San Diego, 1993), vol. 2, pp. 179–220.
 34. T. R. Middendorf, L. T. Mazzola, K. Lao, M. A. Steffen, S. G. Boxer, *Biochim. Biophys. Acta* **1143**, 223 (1993).
 35. The second derivative contribution to the change in absorption, $\Delta A_{\text{Stark}}(\nu)$, in an applied electric field is:

$$\Delta A_{\text{Stark}}(\nu) = (fF_{\text{ext}})^2 \left\{ \frac{C_{\chi}}{30h^2c^2} \frac{\nu d^2[A(\nu)]}{d\nu^2} \right\} \quad (5)$$
 where:

$$C_{\chi} = |\Delta\mu|^2 \{ 5 + (3 \cos^2\chi - 1)(3 \cos^2\zeta_A - 1) \} \quad (6)$$
 h is Planck's constant, C is the speed of light, f is the local field correction factor (36), χ is the experimental angle between the electric vector of the linearly polarized probe light and the direction of the applied electric field, and ζ_A is a molecular angle between $\Delta\mu$ and the transition moment, p . The Stark spectrum in Fig. 2B was obtained at 1.5 K and $\chi = 90^\circ$. The magnitudes of $\Delta\mu$ were calculated from Eqs. 5 and 6 by using values of ζ_A measured in the RC at 77 K. It is unlikely that ζ_A should change significantly at the two temperatures.
 36. The local field correction factor f relates the magnitude of the field present at the chromophore, F_{int} , to that of the externally applied field: $F_{\text{int}} = f \cdot F_{\text{ext}}$. F_{int} is the field due to the external, applied electric field and is not to be confused with the (large) internal electric field that is always present in the RC (or any condensed-phase system) or the additional field $F(P+Q_A^-)$ which results from formation of $P+Q_A^-$. By using the spherical cavity approximation, the local-field correction is given as:

$$f = \frac{3\epsilon}{2\epsilon + 1} \quad (7)$$
 It can be seen that f is only weakly dependent on ϵ . Uncertainties in f do not affect the determination of dielectric asymmetry in these experiments because the local-field correction at the chromophore-protein boundary enters into both the band shift and the determination of $|\Delta\mu|$. Because we take a ratio of expressions that contain these values, this effect cancels. It does, however, play a role in our estimation of the absolute values for ϵ_{eff} . The local field correction also needs to be applied at the protein-solvent boundary, which only enters into the determination of $|\Delta\mu|$. By not accounting for this effect, we are therefore slightly overestimating ϵ_{eff} .
 37. D. S. Gottfried and S. G. Boxer, *J. Lumin.* **51**, 39 (1992).
 38. Stark effect spectra on frozen glycerol/buffer samples at 1.5 K were obtained as described previously (34). Stark spectra for the determination of ζ_A were taken at 77 K in an optical dewar with strain-free windows.
 39. The term $F(P+Q_A^-)$ adds to the intrinsic field in the RC ground state. In order to test whether this affects the values of $\Delta\mu$ for the B and H probe chromophores, the Stark effect spectrum was measured for a sample during actinic irradiation, that is, while the system was in the $P+Q_A^-$ state. The magnitudes of $\Delta\mu$ were found to be within 20 percent of the values obtained for the neutral RC, which is expected because the Stark spectrum has primarily a second-derivative line shape. If these bands had large first-derivative contributions (due primarily to $\Delta\alpha$, the difference polarizability tensor), it is likely that $F(P+Q_A^-)$ would have induced a change in $\Delta\mu$. The Stark line shapes for the Q_y band of P and the Q_x bands of all of the chromophores are more complex, as discussed in detail elsewhere (21, 34); these bands are not relevant to the present discussion.
 40. J. Breton, in *Antennas and Reaction Centers of Photosynthetic Bacteria*, M. E. Michel-Beyerle, Ed. (Springer-Verlag, Berlin, 1985), pp. 109–121.
 41. D. H. Oh, thesis, Stanford University (1991).
 42. H. A. Frank and M. L. Aldema, in *The Photosynthetic Bacterial Reaction Center II—Structure, Spectroscopy and Dynamics*, J. Breton and A. Vermeglio, Eds. (Plenum, New York, 1992), pp. 13–20.
 43. C. Kirmaier, D. Gaul, R. DeBey, D. Holten, C. C. Schenck, *Science* **251**, 922 (1991). The (M)L214H strain, also known as the β mutant, was kindly provided by C. Schenck. This mutant incorporates a BChl a molecule in the place of BPheo a at the H_L binding site, which is useful for the present study because of the enhanced spectral resolution of BPheo bands in the Q_y region (compare Figs. 3A and 4A).
 44. R. K. Clayton and S. C. Straley, *Biophys. J.* **12**, 1221 (1972).
 45. The desirable symmetry-related experiment of examining band shifts upon formation of $P+Q_B$ can unfortunately not be done because electron transfer from Q_A^- to Q_B does not occur at cryogenic temperatures.
 46. The analysis assumes that the upper exciton component of the Q_y transition of P, thought to absorb around 800 nm (12,500 cm⁻¹) (47), has a small integrated oscillator strength relative to the other absorption features. This is justified by the observation that oscillator strength in this wavelength region is very nearly conserved in the ground state and $P+Q_A^-$ absorption spectra, and it is consistent with most calculations.
 47. X. Xie and J. D. Simon, *Biochim. Biophys. Acta* **1057**, 131 (1991).
 48. P. O. J. Scherer and S. F. Fischer, *ibid.* **891**, 157 (1987).
 49. E. J. P. Lathrop and R. A. Friesner, *J. Phys. Chem.* **98**, 3056 (1994).
 50. The estimates for ϵ_{eff} reflect the dielectric response of the entire protein that surrounds P, Q_A, the probe chromophores, and the pathways connecting them. The estimates should not be thought of as the dielectric response of the protein at the particular location of the probe chromophore. Thus, it would have been surprising if the estimates for ϵ_{eff} would be very different for the two chromophores (B_L and H_L) on the L side, because these two chromophores probe very nearly the same region of the protein. Such agreement would not be expected if the shifts for B_L were due predominantly to changes in excitonic coupling, because the coupling between H_L and P should be much smaller than the coupling between B_L and P.
 51. M. A. Steffen, L. Moore, S. G. Boxer, in preparation.
 52. S. L. Hammes, L. Mazzola, S. G. Boxer, D. F. Gaul, C. C. Schenk, *Proc. Natl. Acad. Sci. U.S.A.* **87**, 5682 (1990).
 53. W. W. Parson and A. Warshel, *J. Am. Chem. Soc.* **109**, 6152 (1987).
 54. J. Eccles, B. Honig, K. Schulten, *Biophys. J.* **53**, 137 (1988).
 55. L. K. Hanson, M. A. Thompson, M. C. Zerner, J. Fajer, in *The Photosynthetic Bacterial Reaction Center—Structure and Dynamics*, J. Breton and A. Vermeglio, Eds. (Plenum, New York, 1988), pp. 355–367.
 56. W. W. Parson, Z. T. Chu, A. Warshel, *Biochim. Biophys. Acta* **1017**, 251 (1990).
 57. M. A. Thompson and M. C. Zerner, *J. Am. Chem. Soc.* **113**, 8210 (1991).
 58. H. Treutlein et al., *Proc. Natl. Acad. Sci. U.S.A.* **89**, 75 (1992).
 59. M. Massimo, J. N. Gehlen, D. Chandler, M. Newton, *J. Am. Chem. Soc.* **115**, 4178 (1993).
 60. O. El-Kabani, C.-H. Chan, D. Tiede, J. Norris, M. Schiffer, *Biochemistry* **30**, 5361 (1991).
 61. J. Kyte and R. F. Doolittle, *J. Mol. Biol.* **157**, 105 (1982).
 62. E. W. Knapp and S. F. Fischer, *J. Chem. Phys.* **87**, 3880 (1987).
 63. J. V. Beitz and J. R. Miller, *ibid.* **71**, 4579 (1979).
 64. D. Grand and A. Bernas, *J. Phys. Chem.* **81**, 1209 (1977).
 65. A. M. Kuznetsov, *ibid.* **96**, 3337 (1992).
 66. D. DeVault, *Quantum-Mechanical Tunneling in Biological Systems* (Cambridge Univ. Press, Cambridge, 1984).
 67. Uncertainties in the relative values of ϵ_{eff} will arise from errors in $|\Delta\mu|$ and $\Delta\nu_{\text{obs}}$. For overlapping bands, positive and negative features of the Stark spectrum may cancel, so that the values of $|\Delta\mu|$ obtained from deconvoluted bands will differ from the values obtained without deconvolution. Analysis of the Stark spectra with and without deconvolution produced values for $|\Delta\mu|$ which in all cases agreed to within 0.6 D/f. In the determination of $\Delta\nu_{\text{obs}}$, the band shifts derived by deconvolution were reproducible to within 10 cm⁻¹ starting the fitting procedure with different initial conditions. Cumulative errors from these two effects were always less than 30 percent. Because of the uncertainties in sample thickness, the absolute values of $|\Delta\mu|$ are uncertain by ~15 percent, but this will not affect the relative values. The uncertainties in ϵ_{eff} do not show a simple dependence on the uncertainties associated with ζ_A because ζ_A enters the problem in a nonlinear fashion (see Eq. 6). Because of this, we chose to calculate ϵ_{eff} for each possible value of ζ_A . The ranges of values in Tables 1 and 2 take this uncertainty into account explicitly. Values of ϵ_{eff} less than 1.0 are obviously not possible, and this indicates that the orientation of $\Delta\mu$ for which these values are obtained are likely not correct.
 68. S. Franzen and S. G. Boxer, *J. Phys. Chem.* **97**, 6304 (1993).
 69. G. R. Fleming, J. L. Martin, J. Breton, *Nature* **333**, 190 (1988).
 70. J. P. Allen, G. Feher, T. O. Yeates, H. Komiya, D. C. Rees, *Proc. Natl. Acad. Sci. U.S.A.* **84**, 5730

- (1987).
71. C. H. Chang, O. El-Kabbani, D. Tiede, J. R. Norris, M. Schiffer, *Biochemistry* 30, 5352 (1991).
72. We thank C. C. Schenk for kindly providing the

(M)L214H strain of *Rb. sphaeroides*, M. Plato for providing calculations on P⁺ charge densities, and A. Shreve for helpful discussion. This work was supported by a grant from the NSF Biophys-

ics Program. M.A.S. is the recipient of an MSTP predoctoral fellowship.

30 August 1993; accepted 7 April 1994

AAAS–Newcomb Cleveland Prize

To Be Awarded for a Report, Research Article, or an Article Published in *Science*

The AAAS–Newcomb Cleveland Prize is awarded to the author of an outstanding paper published in *Science*. The value of the prize is \$5000; the winner also receives a bronze medal. The current competition period began with the 4 June 1993 issue and ends with the issue of 27 May 1994.

Reports, Research Articles, and Articles that include original research data, theories, or syntheses and are fundamental contributions to basic knowledge or technical achievements of far-reaching consequence are eligible for consideration for the prize. The paper must be a first-time publication of the author's own work. Reference to pertinent earlier work by the author may be included to give perspective.

Throughout the competition period, readers are

invited to nominate papers appearing in the Reports, Research Articles, or Articles sections. Nominations must be typed, and the following information provided: the title of the paper, issue in which it was published, author's name, and a brief statement of justification for nomination. Nominations should be submitted to the AAAS–Newcomb Cleveland Prize, AAAS, Room 924, 1333 H Street, NW, Washington, DC 20005, and **must be received on or before 30 June 1994**. Final selection will rest with a panel of distinguished scientists appointed by the editor of *Science*.

The award will be presented at the 1995 AAAS annual meeting. In cases of multiple authorship, the prize will be divided equally between or among the authors.